EM-Based Measurement Fusion for HRR Radar Centroid Processing

Benjamin J. Slocumb[a] and William D. Blair[b]

[a]Numerica Inc., PO Box 271246, Ft. Collins, CO 82527, USA
[b]Georgia Tech Research Institute, Atlanta, GA 30332, USA

ABSTRACT

This paper develops a new algorithm for high range resolution (HRR) radar centroid processing for scenarios where there are closely spaced objects. For range distributed targets with multiple discrete scatterers, HRR radars will receive detections across multiple range bins. When the resolution is very high, and the target has significant extent, then it is likely that the detections will not occur in adjacent bins. For target tracking purposes, the multiple detections must be grouped and fused to create a single object report and a range centroid estimate is computed since the detections are range distributed. With discrete scatterer separated by multiple range bins, then when closely spaced objects are present there is uncertainty about which detections should be grouped together for fusion. This paper applies the EM algorithm to form a recursive measurement fusion algorithm that segments the data into object clusters while simultaneously forming a range centroid estimate with refined bearing and elevation estimates.

Keywords: High Range Resolution Radar, Measurement Fusion, Centroid Processing, EM Algorithm, Target Tracking

1. INTRODUCTION

New electronically scanned array (ESA) radar systems are being developed for air and missile defense applications. Such systems use advanced signal processing to provide high target resolution for the purpose of enhancing the classification, discrimination, and identification capabilities. In these sensor systems, the high range resolution (HRR) is achieved with use of new *wide band* waveforms. With the improvements in resolution it is intended that these sensors will be able to resolve and identify multiple closely spaced objects (CSOs). However, waveform advances alone will not bring about the sought after capabilities because new data segmentation/centroid processing techniques are needed to properly process the data.

For HRR radars, a distinction must be made between a *primitive measurement*, which constitutes a detection in a single range bin and its associated range-bearing-elevation parameters, and an *object measurement*, which is the report that is sent to the data association and target tracking processor. When the range resolution is smaller than the target extent, the target will produce multiple primitive measurements across a segment of range cells (possibly not adjacent) during a single radar dwell. By combining primitives, the radar generates the object measurement. The process of fusing the primitives into objects is accomplished with a *centroid processing algorithm*; in particular, a range centroid is computed to estimate the extended target position. When multiple CSOs are present in the data (e.g., for high debris conditions in BMD), there is an uncertainty in the association of primitives with objects. The primitives first must be parsed with a *data segmentation algorithm* into object clusters, and subsequently processed with a *fusion algorithm*. In practice, the segmentation and fusion are accomplished within one centroid processing algorithm.

The HRR radar centroid processing problem is particularly challenging in the ballistic missile tracking scenario shown in Figure 1. First, the issue of *extended targets* is a problem because there is object size uncertainty. Second, the issue of *merged monopulse measurements* is a problem because the presence of multiple objects in a single range bin causes interference in the monopulse response, which subsequently causes direction of arrival calculation errors. Third, the presence of *closely spaced objects* due to debris, stage separations, or other countermeasures, causes uncertainty as to where one object ends and another starts. All of these issues lead to measurement errors that are detrimental to performance of the target tracking system. This could seriously diminish the capabilities of a missile defense system.

Other author information: Send correspondence to Email: bslocumb@numericainc.com, Telephone: 970-419-8343; Email: dale.blair@gtri.gatech.edu, Telephone: 770-528-7934

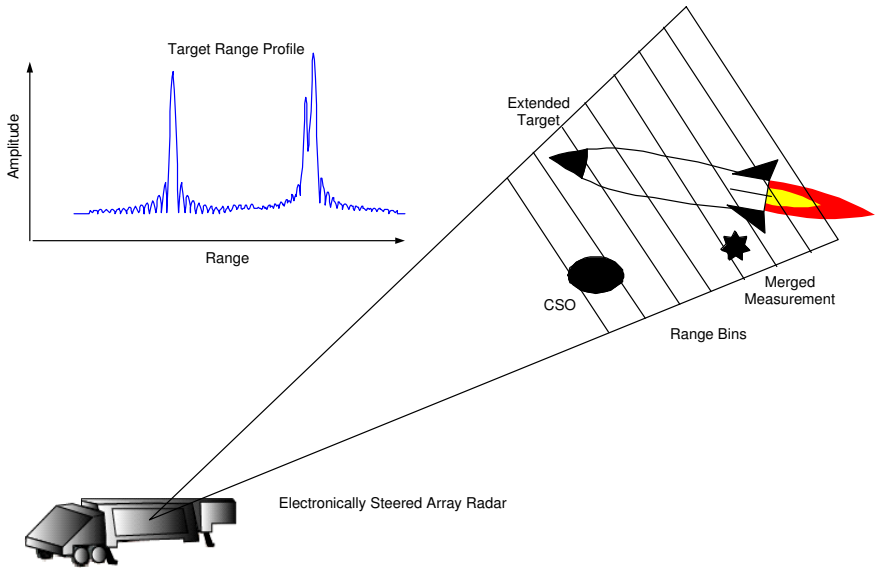

Figure 1: Description of the HRR radar centroid processing problem in ballistic missile tracking.

The topics of HRR radar target response and centroid processing have been treated in the literature, but no research could be identified that addresses the issue of measurement origin uncertainty in the presence of CSOs. Kashyap[1] *et al.* studied the HRR radar range response of missile targets under ideal waveform models, and for realistic cases where clutter, phase noise, and target motion effects degrade the response. Clark[2] developed new HRR radar methods for ballistic missiles that compensate for target motion, in particular target tumbling. Several HRR centroid estimators were described by Hamner and Maier,[3] and simulation results were used to recommend one approach (discussed further later). Recent work by the author[4] developed methods for ESA radar range centroid processing for narrowband waveforms in the presence of CSOs. Also, centroid processing techniques for mechanically scanned surveillance radars have been developed[5]; that problem is related but has somewhat different requirements than the ESA radar centroid processing problem.

This paper is organized as follows. Section 2 describes a number of important aspects of high range resolution radar and its range response to objects with multiple discrete scatterers. Section 3 develops a general measurement fusion algorithm through application of the Expectation Maximization (EM) algorithm for cases where there is uncertainty in the association of the primitive measurements to objects. Section 4 refines the general measurement fusion algorithm for the HRR radar centroid processing problem. Section 5 draws conclusions about the algorithm development.

2. HIGH RESOLUTION RADAR

2.1. Range clustering in electronically scanned array radars

We introduce first some notation for the range centroid processing problem in ESA radars. The radar will make a dwell at time t_k, and with multiple CSOs it will receive detections in a number of range bins. Denote $\{\mathbf{z}_n(t_k); n = 1, \ldots, N\}$ as the set of N primitive measurements received on the dwell, where

$$\mathbf{z}_i(t_k) = [r_i, b_i, e_i, A_i]^T \tag{1}$$

Here, r_i is the range for the bin of the ith primitive, b_i is the bearing, e_i is the elevation, and A_i is the amplitude (or power, or SNR) for the detection received in the ith primitive. Note specifically that primitive measurements from one target may not be adjacent, i.e., that $r_i - r_{i-1} > \Delta r$, where Δr is the range resolution. The presence of "gaps" between primitives makes it more difficult to tell which measurements were from one object.

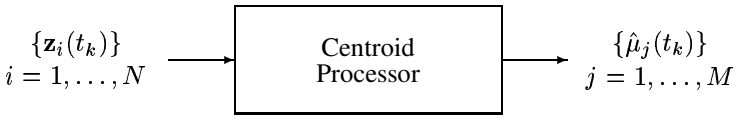

Figure 2: Centroid processor data input/output.

For each primitive measurement, the radar will report an estimate of the measurement covariance, $\mathbf{R}_i$, for the bearing and elevation measurements. As shown in Figure 2, the N primitive measurements are processed by the centroid processing algorithm and create M object measurements ($M \leq N$). The outputs, $\hat{\mu}_j(t_k)$, are the centroid estimates for the jth object. A covariance matrix, Σ_j, will also be generated for the fused measurements.

2.2. Pulse compression waveforms

Each target that a radar engages is composed of multiple discrete scattering points. The reflected energy off each scatterer has its own amplitude, phase, and position. The received signal in a given radar range cell is the coherent sum of the responses of all scatterers within that cell. Target range glint[3] results from fluctuations in the apparent range centroid of scatterers and is due to target movement. This range glint causes higher range variance and subsequently poorer tracking performance of the target.

A way to improve the range measurement accuracy (and target tracking performance) is to use a HRR waveform so that each scatterer on a range-distributed target is isolated into a single range bin. This mitigates the impact of glint, but it also necessitates the need for a *centroid processing algorithm* that combines the multiple scatterer detections into a single object report.

Radar systems achieve high range resolution by using a very narrow pulse width or by using a *pulse compression* waveform. The latter type is generally preferred because a lower transmit power is required for the same detection performance. Pulse compression can be achieved with a variety of modulated waveform types such as those described by Lewis[6] *et al.*: binary phase modulation, step frequency modulation, linear frequency modulation, nonlinear frequency modulation, polyphase modulation, and Huffman and Complementary codes. These waveforms are implemented by modulating the transmitted pulse using a "code," and then processing the return using a matched filter. The major issues in the type selection and implementation are the performance of the range-time sidelobes, and the reception loss associated with target motion (Doppler effects). Both aspects may be characterized by evaluating the ambiguity function for the waveform,

$$AF = |\chi(\tau, f_d)|^2 = \int_{-\infty}^{\infty} s(t)s^*(t-\tau)e^{-j2\pi f_d t}dt \tag{2}$$

where τ is the delay, f_d is the Doppler, and $s(t)$ is the transmitted pulse waveform.

2.3. HRR target profile

For a given radar waveform and target scattering geometry, the HRR target profile is determined by evaluating the ambiguity function along the zero-doppler axis. From Hamner and Maier,[3] the range profile for a HRR radar is given by,

$$A(r) = \left| \sum_{k=1}^{N_s} \chi(\frac{r - r_k}{c}, 0) \right|^2 \tag{3}$$

where r_k is the kth discrete scattering position in range of the object being profiled, N_s is the number of discrete scatterers on the object, and c is the speed of light. Three example ambiguity functions[3] for different wideband waveform types are shown below:

Regular square-pulse (uncompressed) waveform:

$$|\chi(\tau,0)|^2 = \left|\exp(j2\pi f_0\tau)\cdot\left(1-\frac{1}{\tau_p}\right)\right|^2 \tag{4}$$

where f_0 is the RF center frequency and τ_p is the pulse width.

Frequency agile radar, pulse-to-pulse carrier stepped:

$$|\chi(\tau,0)|^2 = \left|\frac{1}{N_f}\sum_{i=1}^{N_f}\exp(j2\pi f_i\tau)\left(1-\frac{|\tau|}{\tau_p}\right)\right|^2 \tag{5}$$

where N_f is the number of step frequencies, and f_i is the RF frequency of the ith pulse, and τ_p is the pulse width.

Step frequency pulse compression waveform:

$$|\chi(\tau,0)|^2 = \left|\sum_{j=1}^{N-n+1} R_{j,j+n-1}(\tau-(n-1)\tau_c,0) \;+\; \sum_{k=1}^{N-n} R_{k,k+n}(\tau-n\tau_c,0)\right|^2 \tag{6}$$

$$n = \lceil|\tau|/\tau_c\rceil, \qquad (n-1)\tau_c \le |\tau| \le n\tau_c \le T_p \tag{7}$$

Here, $R_{jk}(\tau, f_d)$ is the correlation response between any two subpulses $s_j(t)$ and $s_k(t)$ with frequencies f_j and f_k that make up each pulse,

$$R_{jk}(\tau,0) = e^{j2\pi f_k}e^{j\pi(f_j-f_k)\tau}\left(1-\frac{|\tau|}{\tau_c}\right)\;\text{sinc}\left[\pi\tau_c(f_j-f_k)(1-\frac{|\tau|}{\tau_c})\right] \tag{8}$$

where τ_c is the duration of each subpulse.

The expressions above show that the range profile is composed of the summation of a number of sinc-type functions. The width of the sinc (i.e., the range resolution) depends on the bandwidth, and the ability to resolve the individual scatterers depends on their spatial separation relative to the bandwidth. Peaks in the profile may be close together or separated by a number of bins without detected energy. Thus, the centroid processing algorithm must be able to cluster primitive measurements that may be separated (i.e., not adjacent) from other measurements by a significant number of range bins.

2.4. Range centroid estimation algorithms

To reduce the variance in the target range estimate, and to limit the number of reports per object to one, a range centroid is computed for all the primitive measurements (i.e., for each scatterer) per object. Several methods for computing the range centroid were compared.[3] The amplitude (power or SNR) weighted range centroid estimate is

$$\hat{R}_{wgt} = \frac{\sum_{i=1}^{N} A_i r_i}{\sum_{i=1}^{N} A_i} \tag{9}$$

where A_i is the amplitude measured in the ith primitive measurement, and N is the number of primitive measurements per target. The end-point range centroid estimate is

$$\hat{R}_{ep} = \frac{r_1 + r_N}{2} \tag{10}$$

where r_1 is the leading edge range and r_N is the trailing edge range. The geometric range centroid estimate is

$$\hat{R}_{geo} = \frac{1}{N}\sum_{i=1}^{N} r_i \tag{11}$$

Based in simulation results for different wideband waveforms and target models with uniformly random placed scattering points, the amplitude weighted range centroid estimate was determined[3] to be the best estimator. Computing this estimator is straightforward, but only if there are no closely spaced objects.

2.5. Monopulse angle processing in HRR

Monopulse is a simultaneous lobing technique[7] for determining the angular location of a source of radiation or of a "target" that reflects part of the energy incident upon it. Because of accuracy benefits of monopulse, most modern radars use this angle processing technique. For cluster modeling purposes, it is important to know that the angular errors in a monopulse radar have Gaussian distributions.

From Blair and Brandt-Pearce,[8] the monopulse ratio has a Gaussian distribution and is given by

$$y_I \sim \mathcal{N}\left(y_I;\ \frac{\Re_1 \eta_1}{\Re_1 + 1}, \sigma_0^2\right) \tag{12}$$

$$\sigma_0^2 = \frac{1}{2\Re_0}\left[\frac{\sigma_d^2}{\sigma_S^2} + \frac{\Re_1 \cdot \eta_1^2}{\Re_1 + 1}\right] \tag{13}$$

where $\Re_0$ is the observed SNR, $\Re_1$ is the Rayleigh target SNR, σ_d^2 is the difference channel noise power, σ_S^2 is the sum channel noise power, and η_1 is the target direction of arrival (DOA). The target angle of arrival (AOA) is a function of the monopulse ratio. The function is nonlinear, but for targets close to the boresight of the beam the AOA is approximately a linear function of the monopulse ratio,

$$\theta \approx \frac{B_{\theta_0}}{k_m} \cdot y_I + \theta_0 \tag{14}$$

where θ_0 is the boresight pointing angle, B_{θ_0} is the beamwidth at θ_0, and k_m is the monopulse slope. Given that the monopulse ratio is Gaussian distributed, then θ is also Gaussian under the approximation in (14).

When two objects are in the same radar range resolution cell (i.e., a merged measurement condition), then the mean value of the monopulse ratio is the SNR-weighted centroid of the two targets,

$$y_I \sim \mathcal{N}\left(y_I;\ \frac{\Re_1 \eta_1 + \Re_2 \eta_2}{\Re_1 + \Re_2 + 1}, \sigma_1^2\right) \tag{15}$$

$$\sigma_1^2 = \frac{1}{2\Re_0}\left[\frac{\sigma_d^2}{\sigma_S^2} + \frac{\Re_1 \eta_1^2 + \Re_2 \eta_2^2 - \Re_1 \Re_2 (\eta_1 - \eta_2)^2}{\Re_1 + \Re_2 + 1}\right] \tag{16}$$

Therefore, in general the presence of two or more targets in a radar range cell will produce a measurement that is the SNR-weighted centroid of the targets; it also has a variance that is higher than that for a single target. The AOA for merged measurements still is Gaussian distributed.

3. MEASUREMENT FUSION AND EM-BASED CLUSTERING

3.1. Measurement fusion

In target tracking, fusion techniques are used to combine information from multiple sensors to create an improved track estimate. Fusion approaches may be broken into two types: track fusion and measurement fusion.[9,10] Measurement fusion can be accomplished[9] through an augmented filter approach or a weighted observation (compression) approach. The two approaches are equivalent and optimal for the case of a linear state and measurement model. The following theorem shows the weighted observation fusion result from Willner[10] *et al.* is optimal.

THEOREM 1. *Given measurements* $\{\mathbf{z}_1, \ldots, \mathbf{z}_N\}$ *with associated covariance matrices* $\{\mathbf{R}_1, \ldots, \mathbf{R}_N\}$*, where the measurements are distributed on* $p(\mathbf{z}_i|\mu, \mathbf{R}_i) = \mathcal{N}(\mathbf{z}_i; \mu, \mathbf{R}_i)$*, then the optimal fused measurement is given by*

$$\boxed{\hat{\mu} = \mathbf{\Sigma} \cdot \sum_{i=1}^{N} \mathbf{R}_i^{-1} \mathbf{z}_i} \tag{17}$$

where the covariance of $\hat{\mu}$ *is given by*

$$\mathbf{\Sigma} = \left[\sum_{i=1}^{N} \mathbf{R}_i^{-1}\right]^{-1} \tag{18}$$

PROOF. *First, form the measurement vector* $\mathbf{Z} = [\mathbf{z}_1^T \ \cdots \ \mathbf{z}_N^T]^T$. *Assuming that the measurements are independent, then the density for* $\mathbf{Z}$ *is given by*

$$p(\mathbf{Z}|\mu, \mathbf{R}_1, \ldots, \mathbf{R}_N) = \prod_{i=1}^{N} p(\mathbf{z}_i|\mu, \mathbf{R}_i) \tag{19}$$

To find the maximum likelihood estimate for μ, *we maximize the log-likelihood function,*

$$\ell(\mu) = \ln(p(\mathbf{Z}|\mu, \mathbf{R}_1, \ldots, \mathbf{R}_N)) = c + \sum_{i=1}^{N} (\mathbf{z}_i - \mu)^T \mathbf{R}_i^{-1} (\mathbf{z}_i - \mu) \tag{20}$$

where c *is a constant not a function of* μ. *Taking the derivative with respect to* μ *we obtain*

$$\frac{\partial \ell(\mu)}{\partial \mu} = -2 \sum_{i=1}^{N} \mathbf{R}_i^{-1} \mathbf{z}_i + 2 \sum_{i=1}^{N} \mathbf{R}_i^{-1} \mu = 0 \tag{21}$$

Solving this expression for μ *gives the estimator shown in (17). The proof that the covariance of* $\hat{\mu}$ *is given by (18) is as follows,*

$$\begin{aligned}
\mathrm{cov}(\hat{\mu}) &= E\{(\hat{\mu} - \mu)(\hat{\mu} - \mu)^T\} && (22)\\
&= E\{[\mathbf{\Sigma} \cdot \sum_i \mathbf{R}_i^{-1} (\mathbf{z}_i - \mu)][\mathbf{\Sigma} \cdot \sum_j \mathbf{R}_j^{-1} (\mathbf{z}_j - \mu)]^T\} && (23)\\
&= \mathbf{\Sigma} \left[\sum_i \sum_j \mathbf{R}_i^{-1} E\left\{ (\mathbf{z}_i - \mu)(\mathbf{z}_j - \mu)^T \right\} \mathbf{R}_j^{-1} \right] \mathbf{\Sigma} && (24)\\
&= \mathbf{\Sigma} \left[\sum_i \sum_j \mathbf{R}_i^{-1} \cdot \delta_{ij} \mathbf{R}_i \cdot \mathbf{R}_j^{-1} \right] \mathbf{\Sigma} && (25)\\
&= \mathbf{\Sigma} && (26)
\end{aligned}$$

3.2. EM-based measurement fusion with measurement origin uncertainty

The fusion solution in (17) is straightforward, provided we know which measurements belong to the same object. We now turn to the problem where we are provided with $\{\mathbf{z}_1, \ldots, \mathbf{z}_N\}$ and $\{\mathbf{R}_1, \ldots, \mathbf{R}_N\}$, but these measurements belong to M objects (M assumed known and $M \leq N$) and the association of measurements to objects is unknown. The problem can be treated as a clustering problem, and the EM algorithm provides an iterative maximum likelihood approach to clustering.

The EM algorithm was introduced by Dempster, Laird, and Rubin[11] as an iterative approach to solving difficult maximum likelihood estimation problems. To use the EM algorithm, the following steps must be applied:

1. Form a complete-incomplete data model. The incomplete data are the observed measurements, while the complete data include additional information that cannot be observed. If the complete data were know, then the maximum likelihood estimation problem would become solvable.
2. Compute the complete data log-likelihood function.
3. Evaluate the expected value (E-step) of the complete data log-likelihood function given the incomplete data and a current parameter estimate.
4. Maximize the expectation (M-step) with respect to the parameter to define a new parameter estimate.
5. Iterate between the expectation and maximization until convergence is achieved.

The key to applying the EM algorithm is in defining the complete data model. We summarize the EM clustering formulation (same as the mixture density forumulation) here as described in Theodoridis and Koutroumbas[12] and in Bilmes.[13] Suppose that we have measurements $\{\mathbf{z}_1, \ldots, \mathbf{z}_N\}$ with covariances $\{\mathbf{R}_1, \ldots, \mathbf{R}_N\}$; these are the incomplete data. The measurements belong to M clusters, and the objective is to estimate the mean of each cluster. However, the assignment of measurements to clusters is unknown. Thus, the complete data for the clustering problem are $\{(\mathbf{z}_i, \mathbf{R}_i, \lambda_{ij}), i = 1, \ldots, N\}$, where the cluster origination indicator is defined as

$$\lambda_{ij} = \begin{cases} 1, & \text{if } \mathbf{z}_i \in \text{ Cluster } j \\ 0, & \text{if } \mathbf{z}_i \notin \text{ Cluster } j \end{cases} \tag{27}$$

The objective in the clustering problem is to estimate the parameter set $\Theta = [\alpha_1, \ldots, \alpha_M, \mu_1, \ldots, \mu_M]$ where $\alpha_j = P(C_j)$ is the *a priori* probability of cluster j, and μ_j is the mean (centroid) of the jth cluster. An estimate of λ_{ij} is produced via the estimation of α_j.

REMARK 1. *Compared to the classical EM clustering problem,[12] in this formulation the covariance of μ_j is not considered an part of the parameter set to be estimated since the set $\{\mathbf{R}_1, \ldots, \mathbf{R}_N\}$ is reported with the measurements.*

E-Step: The expectation of the complete data log-likelihood given the incomplete data and a current estimate of the parameters of interest is

$$Q(\Theta; \Theta^{(n)}) = \sum_{i=1}^{N} \sum_{j=1}^{M} \left(\pi_{ij}^{(n)} \ln(\alpha_j) + \pi_{ij}^{(n)} \ln(p(\mathbf{z}_i | \mathbf{R}_i, C_j, \Theta)) \right) \tag{28}$$

where the current estimate of the expected value of the cluster origination indicator is

$$\pi_{ij}^{(n)} = E\{\lambda_{ij} | \mathbf{z}_i, \mathbf{R}_i, \Theta^{(n)}\} \tag{29}$$

$$= P(C_j | \mathbf{z}_i, \mathbf{R}_i, \Theta^{(n)}) \tag{30}$$

M-Step: The maximization step is to maximize $Q(\Theta; \Theta^{(n)})$ with respect to Θ,

$$\Theta^{(n+1)} = \arg\max_{\Theta} Q(\Theta; \Theta^{(n)}) \tag{31}$$

Therefore, the maximization problem becomes that of solving the following for each $\theta_j \in \Theta$,

$$\frac{\partial}{\partial \theta_j} \left[\sum_{i=1}^{N} \sum_{j=1}^{M} \pi_{ij}^{(n)} \ln(\alpha_j) + \pi_{ij}^{(n)} \ln[p(\mathbf{z}_i | \mathbf{R}_i, C_j, \Theta)] \right] = 0 \tag{32}$$

The solutions for the *a priori* probabilities $\{\alpha_j\}$ are independent of the specific density function $p(\mathbf{z}_i | \mathbf{R}_i, C_j, \Theta^{(n)})$ and are given by

$$\alpha_j^{(n+1)} = \frac{1}{N} \sum_{i=1}^{N} \pi_{ij}^{(n+1)} \tag{33}$$

$$\pi_{ij}^{(n+1)} = \frac{\alpha_j^{(n)} p(\mathbf{z}_i | \mathbf{R}_i, C_j, \Theta^{(n)})}{\sum_{k=1}^{M} \alpha_k^{(n)} p(\mathbf{z}_i | \mathbf{R}_i, C_k, \Theta^{(n)})} \tag{34}$$

The solution for the other parameters in Θ (i.e., μ_j) depend on the specific density function and are given in the following theorem.

THEOREM 2. *Given measurements $\{\mathbf{z}_1, \ldots, \mathbf{z}_N\}$ with covariances $\{\mathbf{R}_1, \ldots, \mathbf{R}_N\}$, which belong to M clusters, the EM measurement fusion algorithm solution for estimation of the cluster means is*

$$\boxed{\hat{\mu}_j^{(n+1)} = \mathbf{\Sigma}_j^{(n+1)} \cdot \sum_{i=1}^{N} \pi_{ij}^{(n)} \mathbf{R}_i^{-1} \mathbf{z}_i} \tag{35}$$

where $\mathbf{\Sigma}_j^{(n+1)}$ is a covariance matrix defined to be

$$\mathbf{\Sigma}_j^{(n+1)} = \left[\sum_{i=1}^{N} \pi_{ij}^{(n)} \mathbf{R}_i^{-1}\right]^{-1} \tag{36}$$

The iterative a priori probability estimate is given by (33),while the iterative association probability estimate is given by (34). The density function for measurement i given that it came from cluster C_j and given current parameter estimates $\Theta^{(n)}$ is

$$p(\mathbf{z}_i|\mathbf{R}_i, C_j, \Theta^{(n)}) = \mathcal{N}(\mathbf{z}_i; \hat{\mu}_j^{(n)}, \mathbf{R}_i) \tag{37}$$

PROOF. *Starting with the M-step of the EM algorithm in (32), the function that needs to be maximized is*

$$\ln[\alpha_j p(\mathbf{z}_i|\mathbf{R}_i, C_j, \Theta)] = \ln(\alpha_j) + c + (\mathbf{z}_i - \mu_j)^T \mathbf{R}_i^{-1} (\mathbf{z}_i - \mu_j) \tag{38}$$

The partial derivative of this density function with respect to μ_j (and removing the terms not a function of μ_j) is

$$\frac{\partial}{\partial \mu_j} \ln[\alpha_j p(\mathbf{z}_i|\mathbf{R}_i, C_j, \Theta)] = -2\mathbf{R}_i^{-1}\mathbf{z}_i + 2\mathbf{R}_i^{-1}\mu_j \tag{39}$$

Now, substitute into (32) to obtain

$$\sum_{i=1}^{N} \pi_{ij}^{(n)} \left(-2\mathbf{R}_i^{-1}\mathbf{z}_i + 2\mathbf{R}_i^{-1}\mu_j\right) = 0 \tag{40}$$

Solving this equation for μ_j gives the result in (35).

The value of $\mathrm{cov}(\hat{\mu}_j^{(n+1)})$ is not necessarily given by $\mathbf{\Sigma}_j^{(n+1)}$, however (35) and (36) are exactly the Covariance Intersection[14] formulas. Because of this, the consistency condition applies, $\mathbf{\Sigma}_j^{(n+1)} - \mathrm{cov}(\hat{\mu}_j^{(n+1)}) \geq 0$, i.e. the difference is a positive semi-definite matrix. Hence, then $\mathbf{\Sigma}_j^{(n+1)}$ is a conservative upper bound estimate for $\mathrm{cov}(\hat{\mu}_j^{(n+1)})$. The extension of the consistency proof[14] to show it scales from two measurements to N measurements has been shown by Niehsen and Bosch.[15]

REMARK 2. *Equations (35) and (36) are exactly like the measurement fusion equations in (17) and (18) but where the association probability $\pi_{ij}^{(n)}$ is used as a weight in the calculation.*

REMARK 3. *Equations (35) and (36) are the Covariance Intersection formulas[14] where the the ω_i parameters are the association probabilities $\pi_{ij}^{(n)}$. Hence, the covariance estimate is robust to unknown correlations among the measurements, and the estimate $\hat{\mu}_j^{(n)}$ is consistent.*

REMARK 4. *The recursive estimate in (35) has a similar form to the Joint Probabilistic Data Association Filter state estimate. The weights $\pi_{ij}^{(n)}$ are computed in a similar manner to the weights β_{ij} in the JPDAF. Hence, the EM measurement fusion algorithm can be considered a soft association scheme for measurement-to-measurement association, whereas the JPDAF is a soft association scheme for measurement-to-track association.*

4. HRR RADAR CENTROID PROCESSING

4.1. EM algorithm extension to include range centroid estimation

The EM-based clustering algorithm described in Section 3.2 will *segmented* the measurements into clusters while computing each cluster mean. To apply this technique to the HRR radar centroid processing problem, we extract the bearing and elevation measurements (b_i, e_i) from $\mathbf{z}_i$; these parameters have Gaussian distributions and have a constant mean per target. The range values, r_i, are distributed over the target and hence do not follow the cluster mean model. By applying the clustering process to the bearing and elevation measurements, we produce $\hat{\mu}_j^{(n)} = [\hat{b}_j^{(n)}, \hat{e}_j^{(n)}]$. But the *range* centroid estimate must have a separate formulation within the EM-based fusion algorithm.

Recall from Section 2.4 that based on simulation results[3] that the HRR amplitude weighted centroid estimate in equation (9) is the best approach for range-distributed targets. But this estimator assumes knowledge of the range bin and object associations. To achieve this, we use the association probability estimates $\pi_{ij}^{(n)}$ provided by the bearing and elevation EM fusion processing to perform "soft segmenting" of measurements within the range centroid calculation. Also, the bearing-elevation fusion processing uses no information about the target extent to limit infeasible associations of primitive measurements to clusters (i.e., measurements in range bins that extend beyond the maximum object length should not be allowed in the same cluster, even in the AZ/EL values are close).

To estimate the object range, we integrate the object cluster association probability into the weighted range centroid estimate,

$$\hat{r}_j^{(n+1)} = \frac{\sum_{i=1}^{N} \pi_{ij}^{(n)} \cdot A_i \cdot r_i}{\sum_{i=1}^{N} \pi_{ij}^{(n)} \cdot A_i} \tag{41}$$

where r_i is the range for the ith primitive, and A_i is the amplitude measured in the ith primitive. Under ideal conditions, $\pi_{ij}^{(n)} \in \{0, 1\}$, and the summation over all N primitives collapses down to a summation over only those measurements that are in the jth cluster.

Exact calculation of $\text{var}(\hat{r}_j^{(n+1)})$ is complicated. A reasonable approximation is to compute a weighted second geometric moment of the primitives,

$$(\sigma_{r_j}^2)^{(n+1)} = \frac{\sum_{i=1}^{N} \pi_{ij}^{(n)} \cdot A_i (r_i - \hat{r}_j^{(n+1)})^2}{\sum_{i=1}^{N} \pi_{ij}^{(n)} \cdot A_i} \tag{42}$$

Using a geometric second moment is appealing in that as the object extent grows, then so does the uncertainty in the centroid estimate. Further, when particular primitive associations become less certain (especially when they fall in between two objects), then the weighting will inflate the range variance. This is desirable because when the primitive associations are uncertain, we accordingly want the uncertainty in the range centroid estimate to increase.

To incorporate the object extent limits into the clustering algorithm, we redefine the cluster membership probability as follows,

$$\pi_{ij}^{(n)} = P(C_j | \mathbf{z}_i, \mathbf{R}_i, \Theta^{(n)}) \cdot 1(r_i | \hat{r}_j^{(n)}, \ell_0) \tag{43}$$

where

$$1(r_i | \hat{r}_j^{(n)}, \ell_0) = \begin{cases} 1, & \text{if } r_i \in [\hat{r}_j^{(n)} - \ell_0/2, \hat{r}_j^{(n)} + \ell_0/2] \\ 0, & \text{otherwise} \end{cases} \tag{44}$$

and where ℓ_0 is the maximum extent of the expected objects. Thus, if the range r_i of the ith primitive measurement is too far from the jth cluster range centroid, $\hat{r}_j$, it will be prevented from associating to the cluster. In the algorithm implementation, it may be beneficial to increase ℓ_0 beyond the exact maximum length to allow some primitives to properly initialize until $\hat{r}_j^{(n)}$ converges toward the proper value. Alternatively, we may systematically decrease $\ell_0^{(n)}$ within the steps of the EM algorithm recursion.

The inclusion of the extent constraint into (44) may lead to situations where $\pi_{ij}^{(n)} = 0, \ \forall j$. This will happen if there are not enough clusters defined (i.e., M is too small). The solution is to increase M, with initial cluster values set to (r_i, b_i, e_i), and then re-run the EM clustering algorithm.

4.2. Algorithm initialization

A key aspect of the EM clustering algorithm is that the number of clusters M (i.e., the number of target/objects) must be pre-specified. However, in realistic scenarios M is not always known. If this number is not accurate, then the algorithm will perform poorly. We outline here several concepts for determining M; the best solution will require experimentation though future simulation work.

- *Tracker Feedback.* In scenarios where objects/targets are not spawned from existing targets (e.g., no debris, expendables, or stage separation), then the number of objects will be known by the tracker. Based on the predicted state estimates, the tracker can predict the number of objects in the radar beam on a given dwell. Through feedback, the expected number can be reported to the centroid processor.

- *Sequential Parsing.* We may be able to initially parse the measurements into clusters by sequentially comparing measurements $\mathbf{z}_i$ and $\mathbf{z}_{i+1}$. One approach is to use a class separability measure such as the Mahalanobis distance,

$$d_{ij} = (\mathbf{z}_i - \mathbf{z}_j)^T (\mathbf{R}_i + \mathbf{R}_j)^{-1} (\mathbf{z}_i - \mathbf{z}_j) \tag{45}$$

  or the Kulback-Liebler divergence measure,[12]

$$d_{ij} = \frac{1}{2}\mathrm{tr}\left(\mathbf{R}_i^{-1}\mathbf{R}_j + \mathbf{R}_j^{-1}\mathbf{R}_i - 2\mathbf{I}\right) + (\mathbf{z}_i - \mathbf{z}_j)^T (\mathbf{R}_i^{-1} + \mathbf{R}_j^{-1})(\mathbf{z}_i - \mathbf{z}_j) \tag{46}$$

- *Mixture Density Order Determination Methods.* A number of methods for estimating the optimal value for M in the EM algorithm have been published. The Bayesian Information Criterion[16] (BIC) minimizes a negative penalized log likelihood. The Agglomerative Gaussian Mixture Decomposition (AGMD) algorithm[17] operates by partitioning the data into a large number of clusters and then iterating and forcing neighboring clusters to compete. As fewer clusters are modeled, an optimal number is derived.

The final process for the HRR radar centroid processing algorithm may include several of these techniques. Future research and experimentation is required.

5. CONCLUSIONS

This paper has developed a new algorithm for high resolution radar centroid processing. The challenge in this application centers the fact that HRR radars produce multiple detections over a sequence of range bins when engaging range-distributed targets. When there are multiple closely spaced objects (CSOs), which is common in ballistic missile tracking scenarios, there can be significant uncertainty as to which detections (i.e., primitive measurements) should be associated with each object. An Expectation Maximization-based measurement fusion algorithm was derived that iteratively computes estimates of the primitive-to-object association probabilities, along with bearing and elevation estimates for each object. A novel extension includes the amplitude weighted range centroid estimate with the bearing and elevation fusion iterations. The remaining work includes a full simulation development to demonstrate the methodology, continued development of the algorithm initialization procedure, and incorporation of a merged measurement statistical model into the centroid processing algorithm.

REFERENCES

1. S. Kashyap, J. Stanier, G. Painchaud, and A. Louie, "Radar response of missile-shaped targets," *Antennas and Propagation Society International Symposium* **4**, pp. 1910–1913, 1995.
2. M. E. Clark, "High range resolution techniques for ballistic missile targets," *High Resolution Radar and Sonar Colloqium* **1**, pp. 6/1–6/13, 1999.
3. C. A. Hamner and M. W. Maier, "Methods to reduce range glint in radars," *IEEE Aerospace Conference* **3**, pp. 83–102, 1997.
4. B. J. Slocumb, "Default test article ESR centroid processing algorithm," Appendix F, in Functional Description of the Ballistic Missile Defense (BMD) Benchmark Environment, Georgia Tech Research Institute, January 2002.
5. B. J. Slocumb, "Surveillance radar range-centroid processing," *Proceedings of the SPIE, Conference on Signal and Data Processing of Small Targets* **4473**, 2001.
6. B. L. Lewis, F. F. Kretschmer, and W. W. Shelton, *Aspects of Radar Signal Processing*, Artech House, Norwood, MA, 1986.
7. S. Sherman, *Monopulse Principles and Techniques*, Artech House, Dedham, MA, 1984.
8. W. D. Blair and M. Brandt-Pearce, "Unresolved Rayleigh target detection using monopulse measurements," *IEEE Trans. on Aerospace and Electronic Systems* **34**, pp. 543–551, April 1998.
9. Q. Gan and C. J. Harris, "Comparison of two measurement fusion methods for Kalman-filter-based multisensor data fusion," *IEEE Trans. on Aerospace and Electronic Systems* **37**, pp. 273–280, January 2001.
10. D. Willner, C. B. Chang, and K. P. Dunn, "Kalman filter algorithms for multi-sensor system," *Proceedings IEEE Conference on Decision and Control* , pp. 570–574, December 1976.

11. A. P. Dempster, N. M. Laird, and D. B. Rubin, "Maximum likelihood estimation from incomplete data via the EM algorithm," *J. Royal Statistical Society, Serial B* **39**, 1977.
12. S. Theodoridis and K. Koutroumbas, *Pattern Recognition*, Academic Press, San Diego, CA, 1999.
13. J. A. Bilmes, "A gentle tutorial of the EM algorithm and its application to parameter estimation for Gaussian mixture and hidden Markov models," Technical Report TR-97-021, Department of Electrical Engineering and Computer Science, University of California, Berkeley, CA 94704, April 1998.
14. S. J. Julier and J. K. Uhlmann, "A non-divergent estimation algorithm in the presence of unknown correlations," *Proceedings of the American Control Conference* , pp. 2369–2373, 1997.
15. W. Niehsen, "Information fusion based on fast covariance intersection filtering," *Submitted Preprint, International Conference on Information Fusion* , July 2002.
16. G. McLachlan and D. Peel, *Finite Mixture Models*, John Wiley & Sons, New York, 2000.
17. S. Medasani and R. Krishnapuram, "Determining the number of components in Gaussian mixtures using agglomerative clustering," *International Conference on Neural Networks* **3**, pp. 1412–1417, 1997.